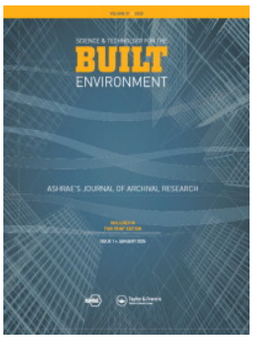

Taylor & Francis
Taylor & Francis Group

Science and Technology for the Built Environment

ISSN: (Print) (Online) Journal homepage: www.tandfonline.com/journals/uhvc21

Development of near-optimal advanced control sequences for chiller plants with water-side economizers in U.S. Climates (ASHRAE RP-1661)

Cary A. Faulkner, Julia Ho, Chengnan Shi, Chengliang Fan, Nasim Ildiri & Wangda Zuo

To cite this article: Cary A. Faulkner, Julia Ho, Chengnan Shi, Chengliang Fan, Nasim Ildiri & Wangda Zuo (2025) Development of near-optimal advanced control sequences for chiller plants with water-side economizers in U.S. Climates (ASHRAE RP-1661), Science and Technology for the Built Environment, 31:1, 18-35, DOI: 10.1080/23744731.2024.2404814

To link to this article: https://doi.org/10.1080/23744731.2024.2404814

Published online: 23 Oct 2024.

Science and Technology for the Built Environment, (2025) **31**, 18–35

ISSN: 2374-4731 print / 2374-474X online
DOI: 10.1080/23744731.2024.2404814

Development of near-optimal advanced control sequences for chiller plants with water-side economizers in U.S. Climates (ASHRAE RP-1661)

CARY A. FAULKNER[1], JULIA HO[2], CHENGNAN SHI[1], CHENGLIANG FAN[1], NASIM ILDIRI[1] and WANGDA ZUO[2,3]*

[1]*University of Colorado Boulder, Boulder, CO, USA*
[2]*The Pennsylvania State University, University Park, PA, USA*
[3]*National Renewable Energy National Laboratory, Golden, CO, USA*

Various advanced control sequences for chiller plants with water-side economizers (WSE) have been proposed in literature, but the evaluation and optimization of those controls is limited. It is possible to maximize energy savings by selecting different sequences and related parameters based on the plant configuration, load, and climate. This paper addresses this gap by developing near-optimal advanced control sequences for chiller plants with WSEs. First, advanced control sequences for chiller plants with WSEs are categorized into condenser water, chilled water, and hybrid controls and representative sequences from each category are identified. Next, 504 different scenarios are optimized. These scenarios represent all possible combinations of two plant configurations, a constant or variable load profile, three advanced control sequences, and seven optimization parameter combinations in six climate zones. The results show the recommended near-optimal sequences can reduce energy consumption by up to 15% relative to the baseline depending on the configuration, load profile, and climate. Specifically, the CW-CHW sequence is recommended for the majority of systems because it is often the most energy efficient and/or reduces the runtime of chillers. The methodology in this paper provides practical guidance for achieving energy savings through near-optimal control of chiller plants with WSEs.

1. Introduction

Chiller plants with water-side economizers (WSEs) can efficiently cool buildings by using free cooling to provide chilled water (CHW) to buildings (Agrawal, Khichar, and Jain 2016). Rather than only using mechanical cooling from chillers, WSEs use free cooling provided by the ambient environment via cooling tower systems to remove heat from the CHW returning from buildings (Energy Star 2024). The control of these systems is critical to their performance (Kim et al. 2021), including when to enable or disable WSEs.

Previous works have studied optimization and control of chiller plants with WSEs (Griffin 2015b; Taylor 2014). Kim et al. (Kim et al. 2021) studied a data center in Korea supplied by a chiller plant with WSE and found that energy could be decreased by 30.1% when CHW temperature differential was modulated for efficient WSE operation. Durand et al. (Durand-Estebe et al. 2014) proposed a temperature adaptive control strategy integrated with a chiller plant with WSE system that provided up to 17% energy savings with low maintenance costs. Another study (Li and Li 2020) optimized the wet bulb temperature condition to switch cooling modes and the cooling tower approach temperature under part load conditions. The optimization results showed cooling system energy savings of 10% when the cooling load ratio is 0.6, and that approach temperature optimization is especially helpful at low cooling load ratios. Fan et al. (Fan et al. 2021) created open source Modelica models for chiller plants with WSE, and demonstrated the models using two advanced control strategies. Most recently, a study (Fan and Zhou 2023) using model predictive control optimization for a chiller plant with WSE found that optimizing condenser water (CW) pump speed saved about 12% energy, while additionally

Received March 29, 2024; accepted August 19, 2024
Cary A. Faulkner, PhD, Student Member ASHRAE, is a Research Engineer. **Julia Ho, BS, Student Member ASHRAE,** is a PhD student. Chengnan Shi, MS, is a PhD student. **Chengliang Fan, PhD,** is an Assistant Professor. **Nasim Ildiri, MS,** is a PhD student. **Wangda Zuo, PhD, Full Member ASHRAE,** is a Professor.
*Corresponding author e-mail: wangda.zuo@psu.edu

optimizing cooling tower approach temperature only improved energy use by about 1.4%.

Despite significant progress in the literature, some research gaps for studying advanced controls of chiller plants with WSE exist. First, there is a lack of comprehensive evaluation and optimization of advanced control strategies for chiller plants with WSE, as most research tends to focus on specific use cases. Second, the relative efficacy of advanced control strategies for systems with different configurations, load profiles, and climates is not well quantified. Finally, more research on advanced controls that chiller plant operators can practically implement is needed. For example, although wet bulb temperature measurements are often used for chiller plant controls in simulation studies (Fan et al. 2021; Fan and Zhou 2023; Li and Li 2020), they are not widely adopted in practice because of measurement error. In addition, prescribed near-optimal rule-based controls can be more practical for operators to implement and maintain compared to other advanced controls that require the development and integration of complex models, such as model predictive controls.

This paper addresses the aforementioned gaps by developing near-optimal advanced control sequences for chiller plants with WSEs. This is accomplished by first reviewing and categorizing advanced control sequences for chiller plants with WSE systems and selecting a representative sequence from each category. Next, a new condenser water supply temperature (CWST) control is proposed that uses cooling tower efficiency rather than wet bulb temperature measurements. Three critical control parameters are then selected to be optimized for the three advanced control sequences (CHW, CW, and hybrid CW-CHW controls), two plant configurations (parallel and series), two load profiles (constant and variable load), and six climates. The results are analyzed in terms of energy performance, free cooling hours, and new metrics describing the WSE potential based on climate and system setpoints. Finally, near-optimal sequences are recommended based on deep analysis of the optimizations and are designed to be as practical and uniform as possible to ease the implementation process for operators. The recommended near-optimal sequence results are compared against true-optimal results conducted in previous work (ASHRAE 2023).

The specific scientific contributions of this paper include: 1) providing a comprehensive optimization study for chiller plants with WSEs to determine near-optimal control sequences through optimizing 504 scenarios including seven combinations of parameter optimizations, three advanced control strategies, two system configurations, two load profiles, and six climates; 2) analyzing the relative efficacy of selected control sequences for different climates, configurations, and load profiles; and 3) identifying three critical control parameters for optimization, including one used for a new method to reset CWST by avoiding wet bulb temperature measurements to improve real-world implementations.

The remainder of this paper is organized as follows. The identified advanced controls, local controls including the new CWST control, and critical control parameters are summarized in Section 2. Next, the methodology to develop near-optimal sequences is described in Section 3. Section 4 then summarizes the identified near-optimal sequences for different scenarios and provides detailed analysis and discussion. Finally, conclusions are drawn in Section 5.

2. Chiller plants with WSE controls

This section introduces the controls for chiller plants with WSE. First, an overview of configurations for chiller plants with WSE is provided. Next, advanced control sequences for these systems are reviewed before identifying three sequences for this study. Then, typical local controls are described including a new CWST reset control. Finally, the critical control parameters to be optimized in this study are identified and summarized.

2.1. Typical configurations of chiller plants with WSE

To better understand the advanced control sequences for chiller plants with WSE, two typical plant configurations are shown in Figure 1. Figure 1a shows a typical configuration with the WSE in parallel with the chillers on the CW side. For this configuration, the CW can flow through the WSE and the chillers in parallel when both are enabled. In contrast, Figure 1b shows a typical configuration where the WSE and the chillers are in series, meaning the CW can flow through the WSE and then the chillers during a single loop when both are active. In both configurations, the CW and/or CHW can bypass either piece of equipment, meaning that the system can operate with just the chillers, both the chillers and WSE, or just the WSE. Additionally, the WSE and chillers are connected in series in the CHW loop for both configurations. Other configurations exist for chiller plants with WSE, such as nonintegrated systems where WSE and chillers cannot be used simultaneously.

2.2. Categorization of advanced control sequences

Numerous advanced control sequences for chiller plants with WSE systems have been found in the literature and can be categorized into CHW, CW, hybrid CHW-CW, and outdoor air temperature based controls. An example of CHW-based controls where only CHW measurements are used for sequencing is described in Taylor (2014). This sequence compares the actual CHW return temperature to the predicted CHW temperature leaving the WSE to determine if the WSE can cool the CHW satisfactorily. Similarly to the CHW-based controls, CW-based controls use CW measurements for sequencing (Meakins 2011; Stein 2009). Meakins (Meakins 2011) proposed activating the WSE when the CW temperature fell below a threshold, while Stein (Stein 2009) manipulated the CW setpoint to maximize the efficiency of the overall chiller plant.

Others adopt a hybrid approach by using a combination of CW and CHW measurements (Comperchio and Behere 2015; Griffin 2015a; Ham and Jeong 2016). For example, one study (Ham and Jeong 2016) suggested activating the WSE when the difference between the CHW return and CW supply temperatures was above a defined threshold. Finally, many chose to sequence WSEs based on outdoor air temperature measurements (Carrier Corporation 2016; Greeley 2006; Jaramillo, Jeon, and

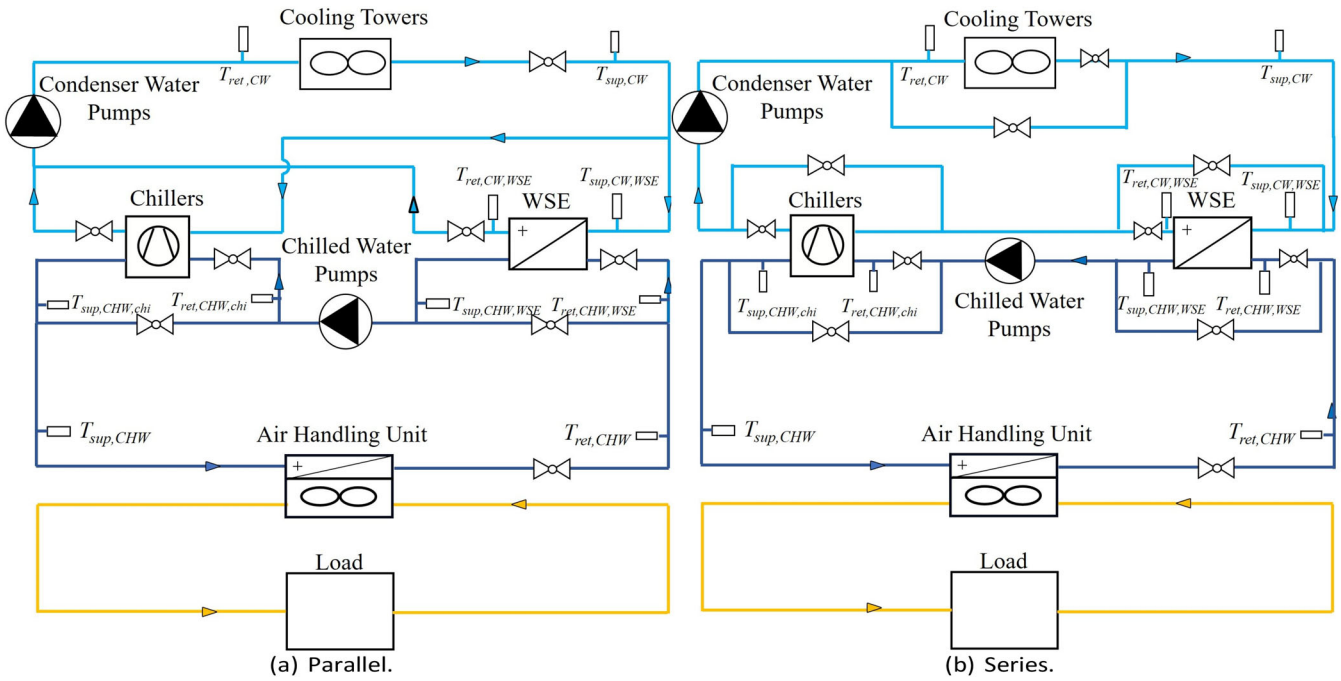

Fig. 1. Typical configurations of chiller plant systems with WSE integrated on the CW side.

Schuster 2015; Kim et al. 2017; Lui 2010; Udagawa et al. 2010). Some used outdoor air temperature in relation to the chilled water setpoint (Carrier Corporation 2016) while others based WSE sequencing solely on outdoor wet bulb temperature measurements (Greeley 2006; Jaramillo, Jeon, and Schuster 2015; Kim et al. 2017; Lui 2010).

2.3. Selected advanced control sequences

Nine out of 20 possible control sequences were deemed implementable after eliminating duplicate controls and control sequences with incomplete information. Details of these control sequences can be found in Table 1. Unimplementable control sequences often did not contain enough information to be replicated, as was the case with some outdoor air temperature-based controls (Carrier Corporation 2016; Kim et al. 2017; Udagawa et al. 2010) and some hybrid controls (Comperchio and Behere 2015; Ham and Jeong 2016). In cases where control sequences were effectively identical, as was the case with (Meakins 2011) and (Griffin 2015a), only one control sequence was considered.

Finally, we categorized the control sequences into three groups: CW based control, CHW based control, and hybrid CW-CHW based control. These span three of the main categories of the reviewed advanced control sequences. The outdoor air temperature category is omitted in this study in part because of uncertainty associated with wet bulb temperature measurements. Additionally, the other categories share similarities, particularly using chiller plant system temperature measurements, that help facilitate the analysis in this study.

2.3.1. CW-based control

Figure 2 shows the CW based control for the WSE system. Transitions between free cooling (FC), partial mechanical cooling (PMC), and full mechanical cooling (FMC) are triggered by the combination of two conditions: temperature comparisons and minimum time thresholds. Temperature comparisons are used to determine what combination of equipment is needed to handle a given load. For example, if the chiller system is in FC mode (where the WSE is on and the chillers are off), a CHW supply temperature above its setpoint suggests that the WSE lacks the capacity to completely cool the water and the system should switch to PMC mode by activating chillers. A deadband temperature (ΔT_{db}) is used to prevent frequent switching between modes. Equipment run time is used to avoid cycling, such as rapidly switching chillers on and off due to a condition like temperature change. For the following controls explanation, t_{thr} defines a minimum time threshold that is determined by the control operator for a given control condition. Its value can vary between control conditions and is used to time conditions including temperature, load, equipment status, and differential pressure.

The CW based control transitions from PMC to FMC when the CWST is warmer than the CHW return temperature upstream of the WSE ($T_{ret,CHW,WSE}$). This signifies the WSE cannot cool the returning chilled water. The transition from FMC to PMC occurs when the CW temperature upstream of the WSE is colder than the CHW return temperature upstream of the WSE, since the WSE can provide cooling for the returning CHW. Finally, the system switches from PMC to FC when the CWST upstream of the WSE is lower than the CHW supply temperature. The measured amount of time the chiller has been on and off and the amount of time the WSE has been on or off is denoted in Figure 2 as $\Delta t_{chiller,on}$, $\Delta t_{chiller,off}$, $\Delta t_{WSE,on}$, $\Delta t_{WSE,off}$, respectively.

2.3.2. CHW-based control

Next, the CHW based control is shown in Figure 3. This control follows similar transition patterns as the CW control,

Table 1. The nine potential advanced control sequences.

	Category	Reference	FC to PMC: Enable Chillers	PMC to FMC: Disable WSE	FMC to PMC: Enable WSE	PMC to FC: Disable Chillers
1	CW	(Meakins 2011) (Griffin 2015a)	$T_{sup,CW,WSE} > T_{sup,CHW,set}$	$T_{sup,CW,WSE} > T_{ret,CHW,WSE} + 1.39^{\circ}C$	$T_{sup,CW,WSE} < T_{ret,CHW,WSE} - 1.67^{\circ}C$	$T_{sup,CW,WSE} < T_{sup,CHW,set}$
2	CW	(Lui 2010)	$T_{sup,CW,WSE} > T_{sup,CHW,WSE}$	$T_{sup,CW,WSE} > T_{ret,CHW,WSE}$	$T_{sup,CW,WSE} < T_{ret,CHW,WSE}$	$T_{sup,CW,WSE} < T_{sup,CHW,WSE}$
3	CW	(Greeley 2006)	$T_{wb,OA} > T_{sup,CHW,set} - (T_{app,CT,des} + T_{app,WSE,des})$	$T_{wb,OA} + (T_{app,CT,des} + T_{app,WSE,des}) > T_{ret,CHW,WSE,des}$	$T_{wb,OA} + (T_{app,CT,des} + T_{app,WSE,des}) < T_{ret,CHW,WSE,des}$	$T_{wb,OA} < T_{sup,CHW,set} - (T_{app,CT,des} + T_{app,WSE,des})$
4	CW	(Stein 2009) (Durand-Estebe et al. 2014)	$T_{sup,CW,WSE} > T_{sup,CHW,set}$	$T_{sup,CW,WSE} > T_{ret,CHW,WSE} - 0.28^{\circ}C$	$T_{sup,CW,WSE,pre} < T_{ret,CHW,WSE} - 1.11^{\circ}C$	$T_{sup,CHW,WSE} < T_{sup,CHW,set}$
5	hybrid	PMS [1]	$T_{sup,CHW,WSE} > T_{sup,CHW,set} + 0.56^{\circ}C$ for 15 min or $T_{sup,CHW,WSE} > T_{sup,CHW,set} + 1.67^{\circ}C$ for 15 min	$T_{sup,CHW,WSE} > T_{ret,CHW,WSE} + 1.11^{\circ}C$ for 15 min	$T_{sup,CW,WSE,pre} < T_{ret,CHW,WSE} - 1.11^{\circ}C$	$T_{sup,CHW,WSE} < T_{ret,CHW,set}$ for 5 min
6	hybrid	PMS [1]	$T_{sup,CHW,WSE} > T_{sup,CHW,set} + 1.11^{\circ}C$ for 5 min or $T_{sup,CHW,WSE} > T_{sup,CHW,set} + 2.22^{\circ}C$ for 1 min	$T_{sup,CHW,WSE} > T_{ret,CHW,WSE} - 1.11^{\circ}C$ for 10 min	$T_{sup,CW,WSE,pre} < T_{ret,CHW,WSE}$ for 10 min and $\dot{Q}_{chiller} > \dot{Q}_{chiller,unload,\min} + 10$ tons or $T_{sup,CW,WSE,pre} < T_{sup,CHW,set} - 0.56^{\circ}C$	$T_{sup,CW,WSE,pre} < T_{sup,CHW,set} - 0.56^{\circ}C$ for 15 min and $S_{fan,CT,\max} < 90\%$ for 30 min
7	CHW	PMS [1]	$T_{sup,CHW,WSE} > T_{sup,CHW,set} + 1.11^{\circ}C$ for 5 min or $T_{sup,CHW,WSE} > T_{sup,CHW,set} + 2.22^{\circ}C$ for 1 min	$T_{sup,CHW,WSE} > T_{ret,CHW,WSE} - 1.11^{\circ}C$ for 10 min	$T_{sup,CHW,WSE,pre} > T_{ret,CHW,WSE} - 1.11^{\circ}C$ for 10 min	$T_{sup,CW,WSE} < T_{sup,CHW,set} - 0.56^{\circ}C$ for 15 min and $S_{fan,CT,\max} < 100\%$ for 15 min
8	CHW	PMS [1]	$T_{sup,CHW,WSE} > T_{sup,CHW,set} + 1.11^{\circ}C$ for 5 min or $S_{CHWP} > 99\%$ and $DP_{CHWP} < 0.9 * DP_{CHWP,set}$ for 15 min	$T_{sup,CHW,WSE} > T_{ret,CHW,WSE}$ for 10 min	$T_{sup,CHW,WSE,pre} < T_{ret,CHW,WSE}$	$\dot{Q}_{chiller} < \dot{Q}_{chiller,unload,\min} + \Delta\dot{Q}$ for 15 min, and $T_{sup,CHW,WSE} < T_{sup,CHW,set} - 1.11^{\circ}C$
9	CHW	PMS [1]	$T_{sup,CW,WSE} > T_{sup,CHW,WSE} + 1.11^{\circ}C$ for 15 min	$T_{sup,CHW,WSE} > T_{ret,CHW,WSE} - 0.56^{\circ}C$ for 2 min	$T_{sup,CW,WSE,pre} < T_{ret,CHW,WSE}$	$S_{fan,CT,average} < 65\%$ for 10 min

except CHW temperature measurements are used in this control sequence. Additionally, pump speed, differential pressure across the chilled water loop, and chiller load are also included in the control sequence. The cooling system switches from FC to PMC mode when either 1) the temperature of the CHW supplied by the WSE is warmer than the CHW supply temperature setpoint or 2) the chilled water pump speed (S_{CHWP}) is at full capacity and the pressure drop across the chilled water loop (DP_{CWS}) is less than 90% of the differential pressure setpoint (DP_{set}). This activates the chillers when either the WSE cannot meet the CHW supply temperature setpoint or the CHW pumps operate near their maximum speed to meet the cooling load. The control switches from PMC to FMC when the CHW supplied by the WSE is warmer than the CHW return, since this means the WSE is not cooling the returning CHW. When the predicted temperature of the CHW supplied by the WSE ($T_{sup,CHW,WSE,Pre}$) is cooler than the CHW return temperature, the system switches from FMC to PMC mode. Lastly, the control changes from PMC to FC mode when either 1) the WSE CHW supply temperature ($T_{sup,CHW,WSE}$) is colder than the CHW supply temperature setpointby some deadband temperature or 2) the current cooling load of the chiller ($Q_{chiller}$) is less than the chiller's minimum unloading load ($Q_{\min,unload}$). This is because either the control predicts the WSE can meet the cooling load alone or the chillers load is already very small. In Figure 3, $\Delta t_{FC}, \Delta t_{PMC}, \Delta t_{WSE,on}$, and $\Delta t_{WSE,off}$ are variables representing time spent in free cooling mode, partial mechanical mode, with the WSE on, and with the WSE off, respectively. Similar to the previous control, they are used for some of the control switching conditions to avoid cycling.

2.3.3. Hybrid CW-CHW control

The last control method is the hybrid CW-CHW based control logic, shown in Figure 4. Unlike the previous two controls, the hybrid control introduces a pre-partial mechanical cooling (Pre-PMC) state that buffers the transition to PMC from FMC to ensure that the WSE has the capacity to cool the returning chilled water. The transition from FC to PMC and from PMC to FMC is similar to the chilled water based logic: both require that the CHW supply temperature be greater than a given reference temperature for some Δt_{thr} and that the WSE be running for some some Δt_{thr}. Additionally, the PMC to FC transition resembles the condenser water control: the chillers are disabled when the predicted CW supply temperature upstream of the WSE is colder than the CHW supply setpoint for some Δt_{thr} and the cooling tower fan speed is less than 90% yet another Δt_{thr}.

Transitioning from FMC to PMC, however, requires two steps. First, the chiller system transitions to Pre-PMC by operating in FMC mode for a given amount of time and either 1) predicting CW supply temperature ($T_{sup,CW,WSE,pre}$) that is colder than the CHW return temperature for some time and a chiller load that is slightly above the minimum unloading load to prevent cycling the chiller on/off when it switches modes or 2) predicting a CW supply temperature that is colder than the CHW supply temperature setpoint. Next, it can transition to PMC mode if the CW supply

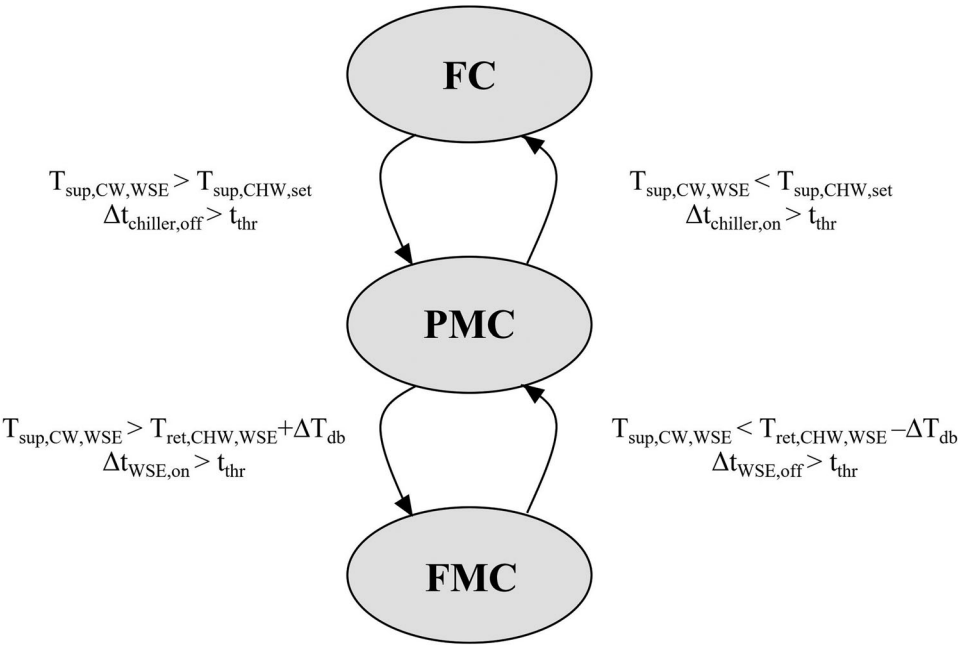

Fig. 2. Condenser water based control logic.

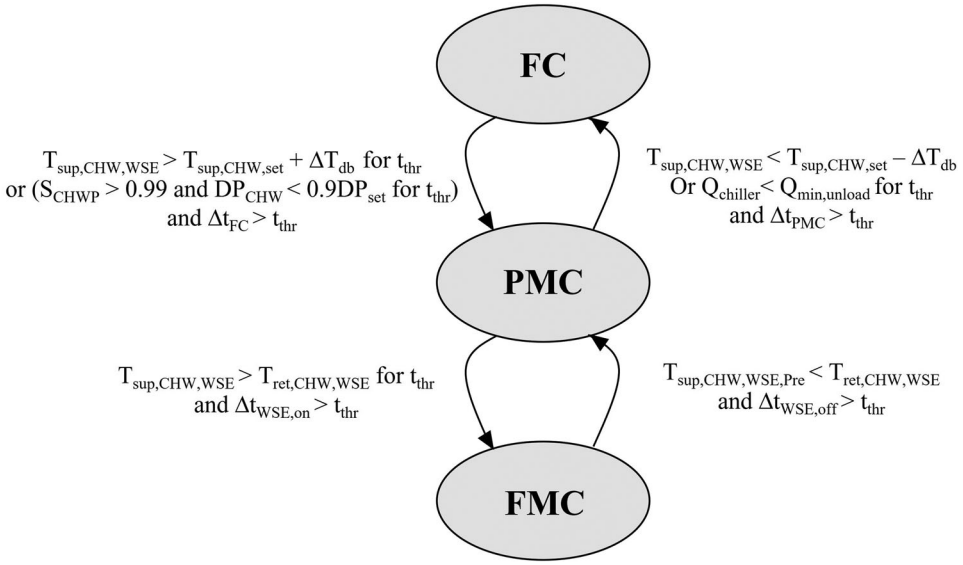

Fig. 3. Chilled water based control logic.

temperature is colder than the CHW return temperature or when the cooling tower fan is not running at full speed ($S_{fan,CT} < 100\%$). If the Pre-PMC to PMC temperature condition is not met and the chiller system has been in Pre-PMC mode for some Δt_{thr}, it transitions back to FMC.

2.4. Local controls

The local controls for the chiller, cooling tower, and pumps are described in this section. These controls were adopted from existing studies for this work.

The chiller local controls focus on staging and depend on the part load ratio (PLR) as opposed to other common metrics such as mass flow or temperature. In FC mode, all chillers are off. In PMC and FMC modes, The PLR at which the chillers are staged on or off is determined by a differential PLR (*dPLR*), as shown in equations 1 and 2 below.

$$PLR_{on} = 1 - dPLR + 0.25, \quad (1)$$

$$PLR_{off} = 1 - dPLR - 0.25, \quad (2)$$

where PLR_{on} is the threshold to stage a chiller on, PLR_{off} is the threshold to stage a chiller off, and *dPLR* is a fixed parameter that can be optimized for energy efficiency. If the PLR_{on} of any chiller is exceeded, the next chiller is staged on. Likewise, chillers are staged off if any chiller's PLR is below the PLR_{off} threshold. Unlike other control methods

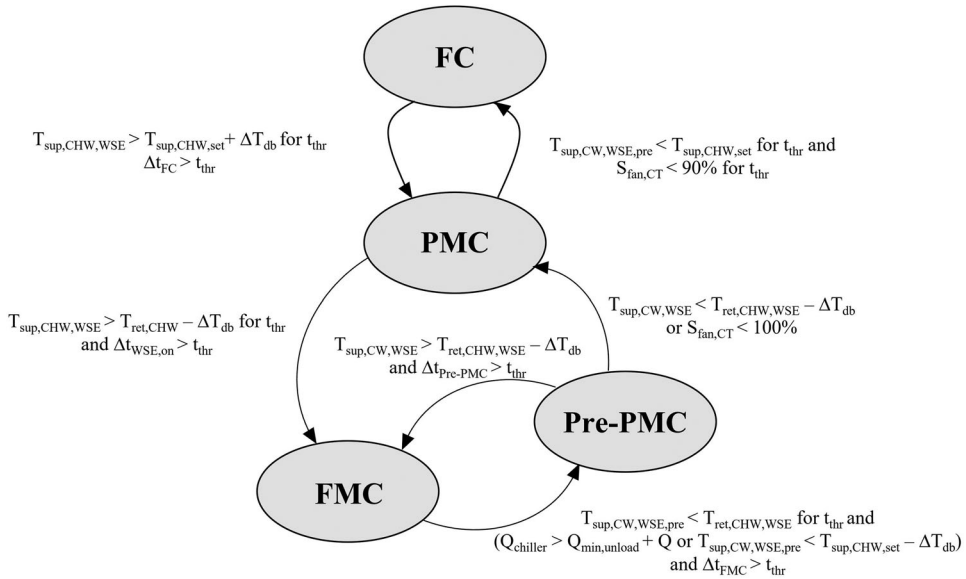

Fig. 4. Hybrid condenser and chilled water based control logic.

that use metrics like mass flow or temperature, PLR control allows the same control commands to be used for both the PMC and FMC modes, thereby simplifying control sequences and facilitating control optimization.

For the cooling tower, local control centers around fan speed. In FC mode, the cooling tower fan speed is controlled to meet the CHW supply setpoint temperature. In PMC and FMC, it is controlled to meet the CW supply temperature setpoint.

Finally, pump local controls consist of staging and speed control. Both pump system controls use pertinent variables within their respective water loops to determine staging and it is assumed variable speed pumps are used. CHW pump staging uses mass flow as a deciding variable, while CW pumps use the cooling tower fan speed for their signal. Both staging controls add buffer times to prevent cycling, and both control their speed using differential pressure setpoints. However, the CW pump also requires the definition of a minimum pump speed to safeguard against freezing water.

2.5. New CWST reset control

A new CWST reset control is proposed to avoid wet bulb temperature measurements and optimize energy use. Because wet bulb temperature calculations are dependent on both dry bulb and relative humidity measurements (Stull 2011), unacceptable amounts of uncertainty and error can be introduced to the system. Therefore, a new method using a measure of cooling tower efficiency is used to reset the CWST setpoint. Although there is also uncertainty associated with cooling tower efficiency measurements, it can be beneficial to control the CWST setpoint by directly monitoring and estimating the system's performance, which wet bulb temperature-based controls do not provide. This control is only used when chillers are activated, since the CWST setpoint is a floating value during FC mode as the cooling tower is controlled to meet the CHW supply temperature setpoint. The logic behind this method is to decrease the CWST setpoint when the cooling tower is operating efficiently, thus shifting the load from the chillers to the cooling tower. Conversely, the CWST setpoint increases when the cooling tower operates inefficiently, so the load shifts from the cooling tower to the chillers.

Trim and respond logic (Taylor 2015) is used to adjust the setpoint based on a critical cooling tower efficiency, kW/ton^{*}_{CT}. The cooling tower efficiency is measured using kW/ton, which is the ratio of electricity consumed by the cooling tower to the cooling load provided by the cooling tower. A high value of kW/ton_{CT} means the cooling tower is operating inefficiently while a lower value means it is operating more efficiently. Thus, the CWST setpoint increases when the cooling tower efficiency exceeds the critical threshold (kW/ton^{*}_{CT}) and decreases otherwise. An example of this control is shown in Figure 5 for a chiller plant with WSE system during a winter day in San Francisco (warm and marine climate). The setpoint increases when the cooling tower efficiency exceeds the critical threshold of 0.1 kW/ton for this case. The increase in setpoint is followed by a drop in the kW/ton as the cooling tower operates more efficiently at the higher setpoint. This can lead to some oscillations in the setpoint as the cooling tower operates near the critical efficiency threshold.

2.6. Critical control parameters for optimization

Three parameters that can improve energy efficiency without sacrificing cooling performance were identified through a literature review. Through the review, it was found that variables that improved energy efficiency in chiller plants with and without WSEs included chilled and condenser water mass flows (Cho and Kim 2016; Taylor 2014), PLR (Ganguly et al. 2016; Wetter et al. 2014), CHW and CW supply temperatures (Carrier Corporation 2016; Udagawa et al. 2010), CHW and CW temperature differentials (Carrier Corporation 2016),

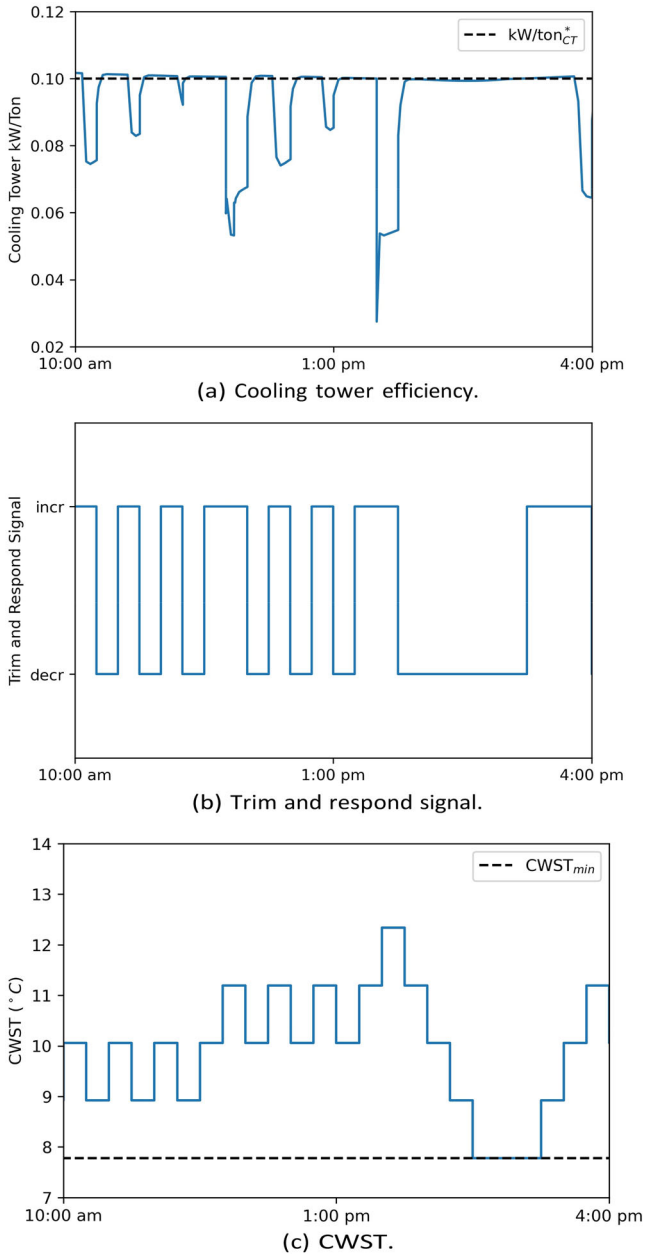

Fig. 5. Example of the new CWST reset control for one day in San Francisco.

supply air temperature (Carrier Corporation 2016; MacQueen 1997), approach temperatures (Li et al. 2014; Zhang et al. 2014), and differential pressures (Huang, Zuo, and Sohn 2017; Park, Clark, and Kelly 1985). In this work, many parameters within the chiller plant are either controlled through operating systems like variable speed drives or have fixed setpoint values to maintain required environmental conditions. For example, supply air temperature and CHW temperature are not manipulated in this work because they can impact the ability to meet the cooling load through the air handling system and this work focuses on the operation of chiller plants with WSEs. Therefore, the most promising optimization variables were narrowed down to those related to the controls of the CWST, PLRs for chiller staging, and temperature differentials used to change between cooling modes. Specifically, the cooling tower efficiency threshold to initiate CW temperature reset kW/ton^*_{CT} (used in the CWST control), the differential PLR to determine chiller staging ($dPLR$), and temperature deadband ΔT_{db} to switch between cooling modes, all have the potential to improve energy efficiency without sacrificing cooling performance. These parameters span several aspects of the system control, including the advanced control to switch between cooling modes and local controls of the cooling tower and chillers.

Firstly, the critical cooling tower efficiency threshold (kW/ton^*_{CT}) is a critical optimization parameter that governs the CWST reset, as described in Section 2.5. The control of the CWST setpoint impacts both the load on the cooling tower and on the chiller, such that a lower setpoint reduces the lift of the chiller but increases the load on the cooling tower, and vice versa for a higher setpoint. Optimizing the kW/ton^*_{CT} can therefore improve the combined efficiencies of the chiller and cooling tower. Secondly, the chiller differential part load ratio ($dPLR$) was chosen as a critical optimization parameter because it influences chiller staging, which can significantly impact chiller energy efficiency (Liu et al. 2017; Seo and Lee 2016). The on and off staging conditions for chillers are determined using $dPLR$ as described in Equations 1 and 2 in Section 2.4. Finally, the deadband temperature range ΔT_{db} controls when the switch from one cooling mode to another occurs. Optimizing this parameter can improve the overall system energy efficiency by operating the system in its most energy efficient cooling mode. As an example, it is used for staging between PMC and FMC modes for the CW control and between PMC, FC, and Pre-PMC modes for the hybrid control. In the hybrid control, the control switches from PMC to FMC when the chilled water supply from the WSE exceeds the chilled water return temperature minus ΔT_{db}.

The selected optimization parameters, their ranges, and their default values are summarized in Table 2. The values and their ranges are chosen based on the engineering judgment of the authors as well as practical limitations (e.g., the range of $dPLR$ is limited considering Equations 1 and 2). Lastly, the range for ΔT_{db} is chosen based on differential temperatures of $[-1.67, 1.67]^\circ$C.

3. Methodology for developing near-optimal controls

3.1. General approach

The goal of this work is to provide near-optimal sequences for chiller plants with WSEs that can be practically implemented to achieve energy savings. These prescribed sequences do not require operators to develop and integrate complex models for their controls. This is accomplished by first defining the approach to optimize the identified critical control parameters for the selected advanced sequences. The optimized results then provide a reference point for developing the near-optimal controls. Additionally, suitable evaluation metrics are required to compare the results and determine the near-optimal sequences. Finally, a wide range of scenarios including different plant

Table 2. Summary of optimization parameters.

Parameter	Description	Range	Default Value
ΔT_{db}	Deadband for switching conditions between cooling modes.	$[-1.67, 1.67]^{\circ}$C	0°C
kW/ton^{*}_{CT}	Critical cooling tower efficiency threshold to begin CWST reset.	[0.025, 0.175] kW/ton	0.1 kW/ton
dPLR	Differential chiller partial load ratio to determine thresholds to stage chillers on or off.	[0.3, 0.5]	0.4

configurations, load profiles, and climates are considered to develop near-optimal sequences for different conditions or understand how the near-optimal sequences can be generalized for different conditions. The near-optimal results are compared against the baseline and true-optimal results to understand their incremental improvements.

3.2. Optimization problem

The chiller plant with WSE system is optimized by minimizing the energy use of the system, described as follows:

$$\begin{aligned} \min_{\mathbf{x}} \quad & \left[E_{chi}(\mathbf{x}) + E_{CT}(\mathbf{x}) + E_{pumps}(\mathbf{x})\right] \\ s.t. \ \ & \mathbf{x} \in \left[\Delta T_{db}, dPLR, \frac{kW}{ton^{*}_{CT}}\right], \\ & -1.67^{\circ}C \le \Delta T_{db} \le 1.67^{\circ}\text{C}, \\ & 0.3 \le dPLR \le 0.5, \\ & 0.025 \le kW/ton^{*}_{CT} \le 0.175. \end{aligned} \tag{3}$$

where x is the set of optimization parameters, E_{chi} is the energy of the chillers, E_{CT} is the energy of the cooling towers, and E_{pumps} is the energy of the CW and CHW pumps. The parameters are optimized within their ranges defined in Section 2.6 for annual simulations. A pattern search optimization algorithm (Moser 2009) is adopted for this study because of its usefulness for multi-parameter optimizations (Han et al. 2021). We compared the use of this optimization algorithm against an exhaustive search when optimizing two parameters. The results showed the optimization algorithm provided almost the same optimal result (<1% difference in energy consumption) as the exhaustive search, but was six times faster. Thus, the pattern search optimization algorithm was adopted for this study.

3.3. Evaluation metrics

The majority of the analysis in this study is based on the annual chiller plant energy consumption, which is used as the objective for the optimization. This includes energy consumption of the chillers, cooling towers, and pumps. The free cooling hours, which is the time the system is in FC mode when all chillers are off, are also used for the evaluation, but not in the optimization problem. This metric is useful for determining the lifespan of chillers, since using chillers less frequently can extend their lifespan.

Additionally, new metrics are created to evaluate the economizing potential of chiller plants with WSE. The metrics are based on the concept of cooling degree days (Energy Information Administration 2023), but applied specifically for chiller plants with WSE systems to describe free cooling potential and how much full mechanical cooling is needed. The first metric is calculated as:

$$FCDD = \int max(CHWST_{set} - T_{wb,oa}, 0)dt, \tag{4}$$

where *FCDD* are "free cooling degree days," $CHWST_{set}$ is the CHW supply temperature setpoint, and $T_{wb,oa}$ is the outdoor air wet bulb temperature. This metric integrates the difference between the CHWST setpoint and the outdoor wet bulb temperature over time to compute the magnitude of potential free cooling based on the climate and system setpoint. This is because free cooling can only meet the CHWST setpoint without chillers when the the outdoor wet bulb temperature is below this setpoint. A higher FCDD means the free cooling potential is greater, which can potentially lead to more energy savings.

The next metric is calculated as:

$$FMCDD = \int max(T_{wb,oa} - CHWRT_{set}, 0)dt, \tag{5}$$

where *FMCDD* is the full mechanical cooling degree days and $CHWRT_{set}$ is the CHW return temperature setpoint (or nominal value). This metric instead determines the magnitude of full mechanical cooling by integrating how much the outdoor wet bulb temperature exceeds the CHWRT over time. This is because the outdoor air cannot cool the returning CHW when the wet bulb temperature is higher than the CHWRT. A higher FMCDD means more mechanical cooling is required, which can potentially lead to higher energy consumption.

3.4. Optimization scenarios

The optimization scenarios are summarized in Table 3. The optimizations are performed for the two configurations, two load profiles, three advanced control sequences, and six climate zones. The configuration of the chiller plant includes the WSE integrated on the CW side either in parallel or in series with the chillers, as described in Section 2.1. Two load profiles are considered: a constant and variable load. The constant load represents a 2,160 kW data center. The variable load represents an office building with an attached data center, the peak load of which is equal to the constant load (2,160 kW). Although the peak load remains the same, the variable load profiles differ for each climate, which are determined using EnergyPlus™. The CW, CHW, or hybrid control sequences described in Section 2.3 are applied for the different system types and load profiles. The simulations are conducted considering six climate zones in the U.S.: 2B (hot and dry), 3 A (warm and humid), 3 C (warm and marine), 4 C (mixed and marine), 5B (cool and dry), or 6 A (cold and humid). The representative cities are Tucson, AZ,

Table 3. Summary of optimization scenarios.

Category	*Values*
Plant configuration	Parallel or series
Load profile	Constant or variable
Control sequence	CW, CHW, or CW-CHW
Climate zone	2B, 3A, 3C, 4C, 5B, or 6A
Optimization combinations	ΔT_{db}, kW/ton^*_{CT}, $dPLR$, ΔT_{db} & kW/ton^*_{CT}, ΔT_{db} & $dPLR$, kW/ton^*_{CT} & $dPLR$, or ΔT_{db} & kW/ton^*_{CT} & $dPLR$

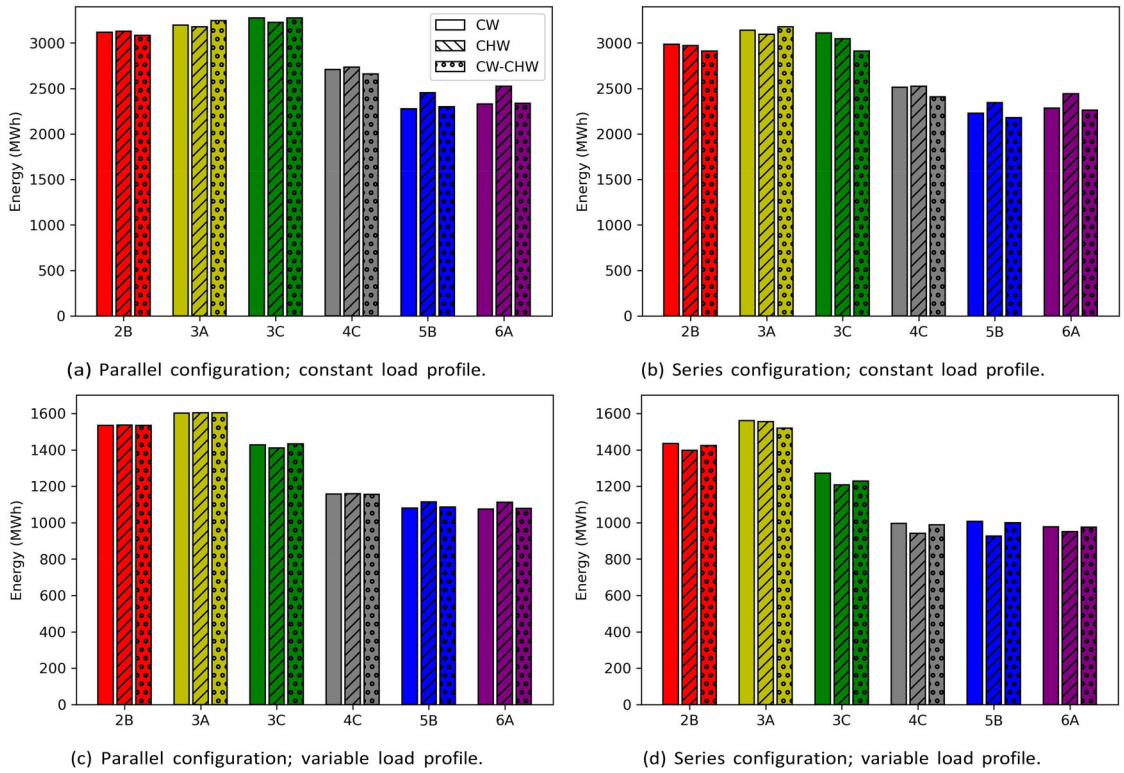

Fig. 6. Baseline energy results for the chiller plants with WSE systems.

Atlanta, GA, San Francisco, CA, Seattle, WA, Denver, CO, and Rochester, MN, respectively. The three optimization parameters described in Section 2.6 are optimized individually, in pairs, or all together, leading to seven different optimization parameter combinations. In total, this results in 504 possible optimization scenarios (2 configurations × 2 load profiles × 3 control sequences × 6 climate zones × 7 optimization parameter combinations).

3.5. Comparison with true-optimal results

The developed near-optimal sequences are compared against true-optimal results, which come from Section 3 of the ASHRAE RP-1661 report (ASHRAE 2023). The same models, plant configurations, load profiles, advanced control sequences, and climate zones are used to determine the true-optimal results. The key difference is the control parameters are optimized at the hourly level throughout the year for the true-optimal scenarios, rather than optimized for one value throughout the year for the near-optimal scenarios. Optimizing the control parameters for each hour throughout the year can yield impressive results, but is not a practical solution for operators to implement. Thus, the true-optimal results are used for comparison purposes only in this paper. The true-optimal results also optimized ΔT_{db} and $dPLR$ using their same ranges in this study, but a parameter different than kW/ton^*_{CT} was used. This parameter was also related to the CWST reset control, but used a different method than that described in Section 2.5.

4. Results

The results are presented and discussed in this section. First, an overview of the baseline and optimized results are analyzed. Then, key results including the optimization of

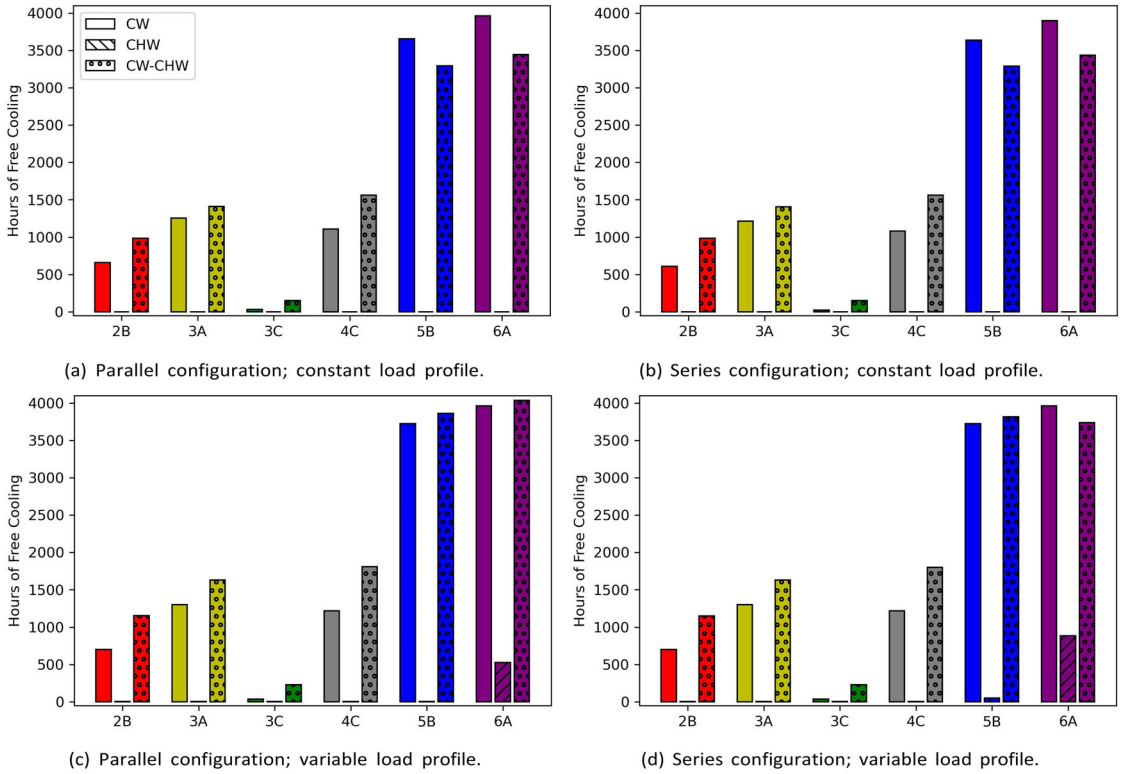

Fig. 7. Baseline hours in FC mode for the chillers plant with WSE systems.

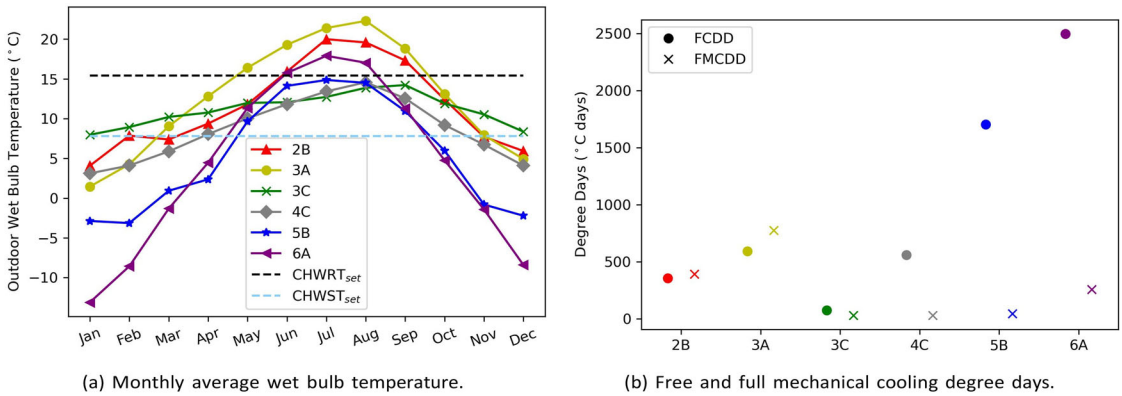

Fig. 8. Monthly average wet bulb temperature and free cooling and full mechanical cooling degree days for each climate.

kW/ton^{*}_{CT} and analysis of the sequences for parallel compared to series configurations for variable load profiles are examined.

4.1. Overview of results

First, a broad overview of the results for the different sequences, configurations, load profiles, and climates are presented. The baseline results are shown first before detailing the optimization results.

4.1.1. Baseline results

The baseline energy results are shown in Figure 6. The results are presented for the six climates and three sequences by dividing the subplots by combination of configuration and load profile. First, the constant load profile cases consume more energy than the variable load profiles cases because the constant load is equal to the peak load from the variable load case, so the total load for the constant load is much higher. Next, the colder climates 4C, 5B, and 6A consume less energy than the warmer climates 2B, 3A, and 3C, because the colder climates can utilize more free cooling. The most energy efficient sequence is dependent on climate, configuration, and load profile. For example, the CHW sequence consumes more energy for the colder climates in all cases except the series configuration and variable load profile case, when it is often the most energy efficient. The series configuration is generally more energy efficient than the parallel configuration for the sequences, climates, and

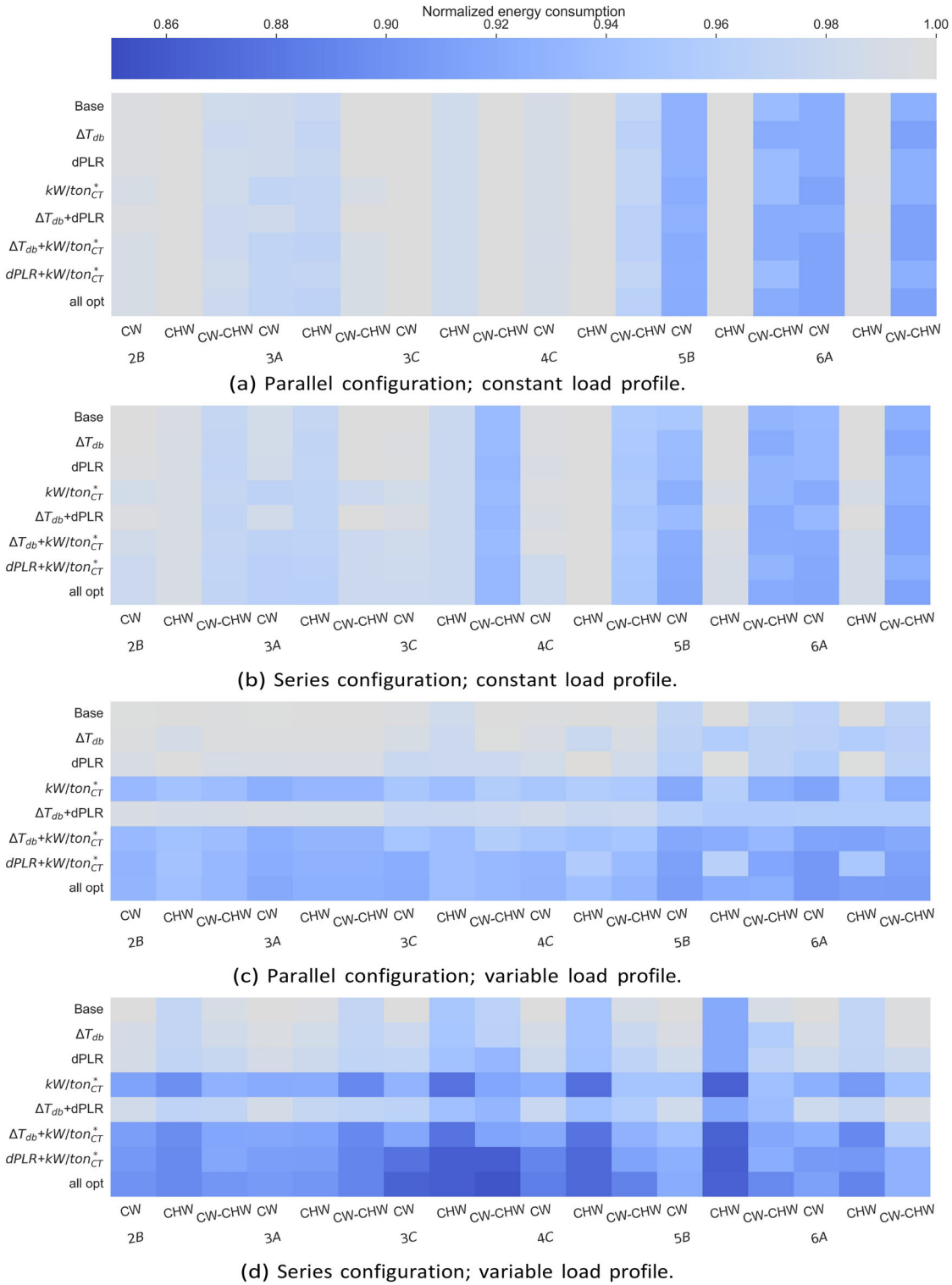

Fig. 9. Optimized energy results for the chiller plants with WSE systems.

load profiles in this study. These savings often come mainly from the CW pump operation, which is shown later in Section 4.2.

Next, the number of hours each system is in FC mode during the year are shown in Figure 7. First, the colder climates are often able to use more free cooling compared to the warmer climates, since the CW can be more efficiently cooled by the outside air in the colder climates. Climate 3C uses the least amount of free cooling, because the temperature remains more constant throughout the year and often does not get cold enough to operate in free cooling mode. The CW-CHW sequence often uses the most free cooling time of the three sequences and the CHW sequence typically uses the least free cooling time. Interestingly, more free

cooling time does not always correlate with less energy consumption. For example, the CHW sequence uses the least free cooling time and consumes the most energy of the three sequences in colder climates for three of the four load cases. However, it consumes the least energy among the three sequences in the colder climates for the series configuration with variable load case, despite still using the least free cooling. This finding is analyzed in more detail in Section 4.2.

The baseline results emphasized the impact of climate on free cooling time and energy use. To explore this impact,

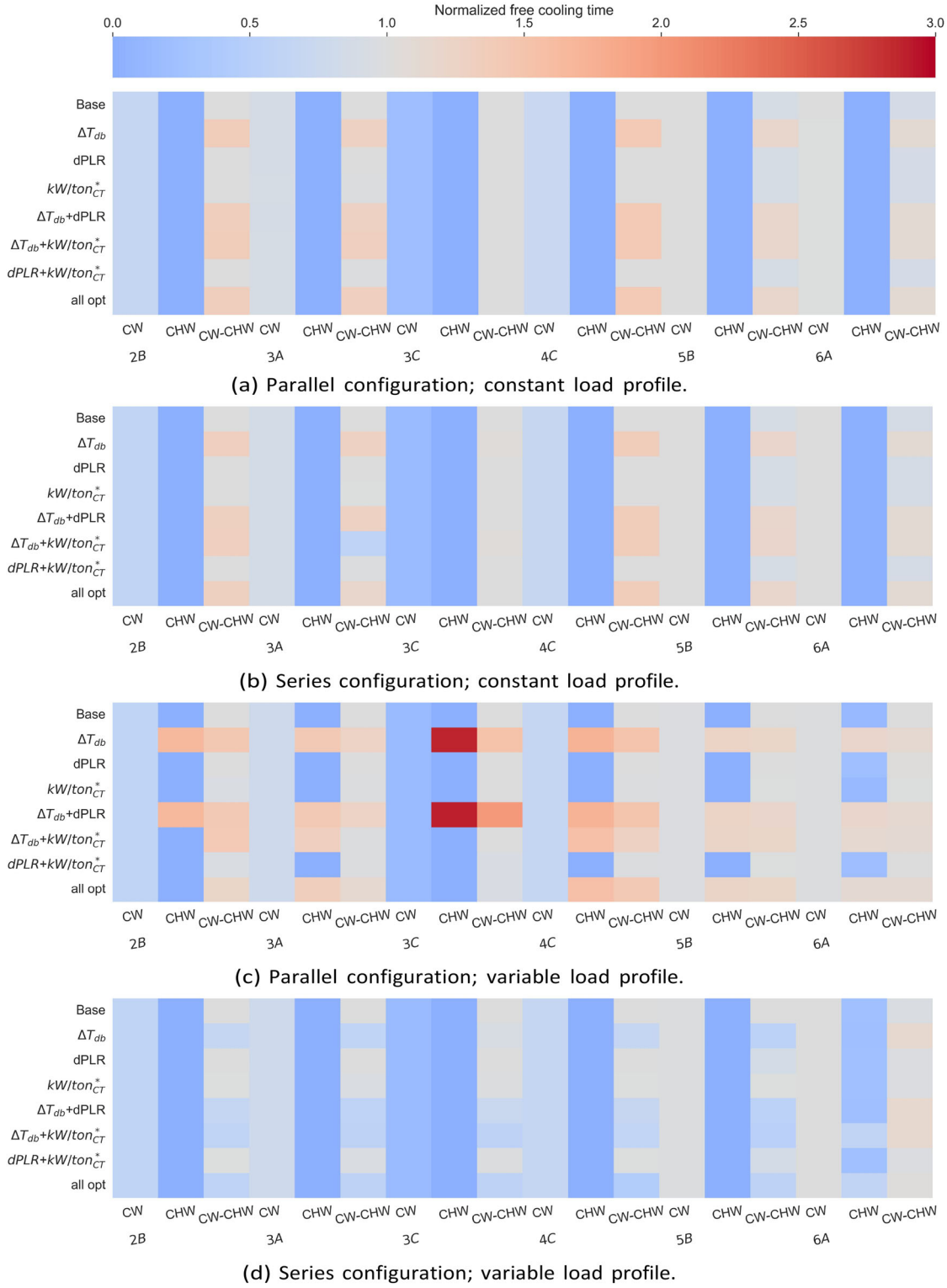

Fig. 10. Hours in FC mode for the optimized results of the chiller plants with WSE systems.

Figure 8 shows the monthly average wet bulb temperature and the computed FCDD and FMCDD (described in Section 3.3) for the six studied climates. The CHWRT and CHWST setpoints are shown as well since these are used to calculate FCDD and FMCDD. These are key setpoints because free cooling alone cannot meet the CHWST setpoint when the outdoor wet bulb temperature exceeds this setpoint. Additionally, the outdoor air cannot cool the CHWRT when the outdoor wet bulb temperature exceeds it, so more FMC mode must be used then.

First, Figure 6 showed that the hot and dry climate 2B often consumed less energy than the warm and humid climate 3A. Figure 8 shows that climate 2B tends to have slightly higher wet bulb temperature winters, but slightly lower wet bulb temperature summers. This is especially because of the humid summers in 3A compared to the drier summers in 2B. Free cooling is less efficient when the air is more humid, which is why 2B can consume less energy than 3A. A similar trend is seen for climates 5B and 6A. For both these cases, the warmer and drier climates (2B and 5B) have lower FCDDs and FMCDDs than the colder and more humid climates (3A and 6A). The systems operate most efficiently for climates with high FCDDs (when more free cooling is used) and low FMCDDs (when less FMC mode is used), but there appears to be a tradeoff when either both are higher or lower.

The previous results also showed that climate 3C used very little free cooling, but consumes less energy than climates 2B and 3A for some conditions. Figure 8 shows that this is because the outdoor wet bulb temperature rarely drops below the CHWST setpoint (meaning free cooling is rarely used), but also rarely exceeds the CHWRT. As a result, the systems frequently operate in PMC mode rather than FC or FMC modes. This is further exemplified by climate 3C having the lowest FCDD and FMCDD. Climates 4C and 5B also have very few FMCDDs, but consume less energy than 3C because of they have more FCDDs.

4.1.2. Optimization results

The optimization results are shown in Figure 9. Each heat map separates the results by sequence and climate zone on the x-axis and by the optimized parameter(s) on the y-axis. The color shows the magnitude of normalized energy consumption, where each case is normalized by the maximum baseline energy consumption among the three sequences for each climate. For example, the results in climate 2B for the parallel configuration and constant load profile case are normalized by the baseline energy consumption for the CHW sequence. Darker blues represent more energy savings relative to the baseline for that climate, and gray colors indicate that the result is closer to the baseline results (i.e., normalized value of 1). The results are separated by combinations of configuration and load profile.

First, optimizing the parameters does not typically show significant savings for the constant load systems. For example, while the CW and CW-CHW sequences are more energy efficient in climate 5B for the parallel configuration and constant load profile case, the differences in energy consumption are not significantly different when optimizing all of the parameters compared to optimizing none of them. However, the optimization is more beneficial for the variable load profile cases, especially with the series configuration. Optimizing kW/ton^{*}_{CT} offers the most energy savings of any

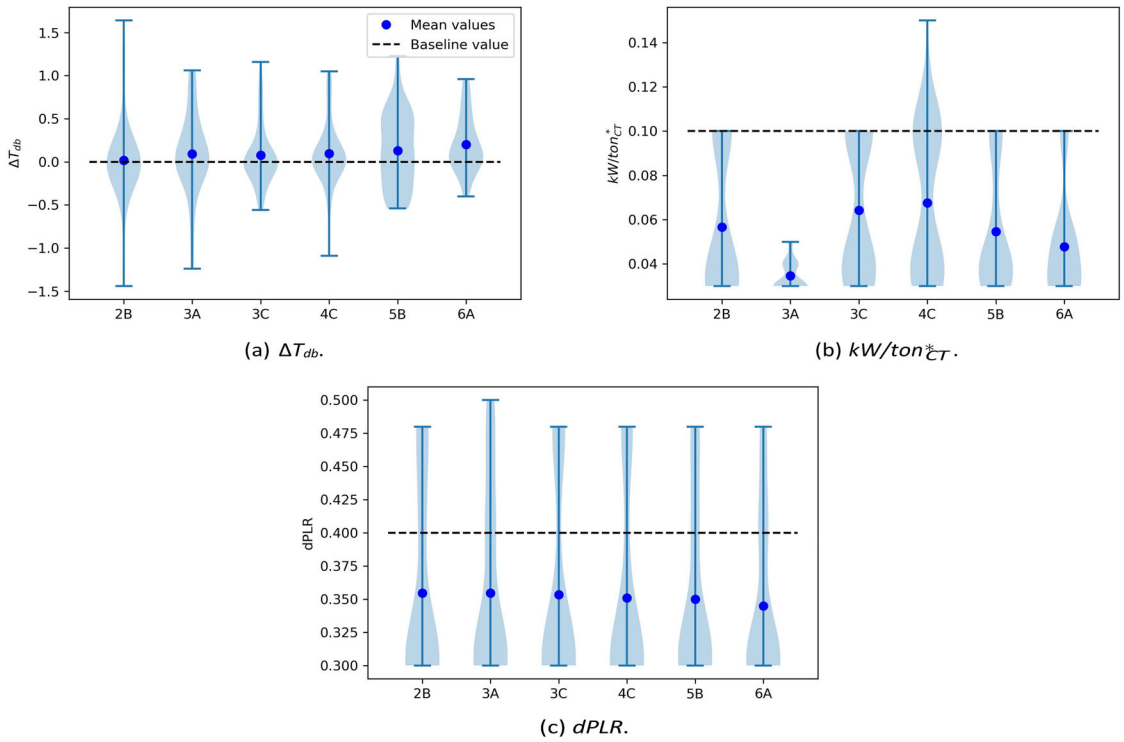

Fig. 11. Distribution of optimized parameter values for each climate.

single parameter for these cases, although further savings can be achieved by optimizing this parameter in combination with the others.

Next, the hours in FC mode are shown for the optimized results in Figure 10. A similar normalization as in Figure 9 is used for these plots, except the optimization cases in each climate are normalized by the maximum FC hours among the three sequences. A red color signifies an increase in FC hours, a blue color represents a decrease in hours, and a gray color is almost no change.

First, optimizing ΔT_{db} (either alone or in combination with other parameters) often increases the FC hours, except for the series configuration and variable load profile cases where it decreases the hours. Optimizing ΔT_{db} most directly impacts the FC hours compared to the other two parameters since this parameter is used for the switching conditions between different modes in each sequence. However, the increase in FC hours from this optimization does not typically significantly reduce energy consumption. For example, optimizing ΔT_{db} for parallel configuration and variable load profile systems can result in up to three times more FC hours, but less than 5% energy savings. Additionally, ΔT_{db} is sometimes optimized to reduce the FC hours and provide a small amount of energy savings for the series configuration and variable profile cases. Lastly, the previous results show optimizing kW/ton^{*}_{CT} for the variable load profile cases can lead to significant energy savings, but optimizing this parameter does not typically impact the FC hours. This is because the parameter kW/ton^{*}_{CT} most directly impacts the operation in PMC and FMC modes rather than the control of the sequences to switch between modes.

Figure 11 shows optimized parameter distributions with respect to climate zone. First, the mean optimized values of the ΔT_{db} distributions are often close to its baseline values, while the mean optimized values of kW/ton^{*}_{CT} and *dPLR* are typically lower than their baseline values. The distributions of kW/ton^{*}_{CT} are often bimodal with one peak around 0.10 and one near 0.04, which correspond to the optimized constant and variable load values, respectively. The distributions of *dPLR* suggest that the optimal values are typically lower than the baseline and the systems tend to operate more efficiently by limiting staging on additional chillers. Lastly, the distributions of ΔT_{db} show the optimal values are almost normally distributed around the baseline values.

Table 4. Recommended advanced control sequence category and optimization parameters to develop near-optimal controls.

Configuration/ load profile	*2B*	*3A*	*3C*	*4C*	*5B*	*6A*
Parallel; Constant	CW-CHW; ΔT_{db}	CW-CHW; ΔT_{db}	CW-CHW; Default Setpoints	CW-CHW; ΔT_{db}	CW-CHW; ΔT_{db}	CW-CHW; ΔT_{db}
Series; Constant	CW-CHW; ΔT_{db}	CW-CHW; ΔT_{db}	CW-CHW; Default Setpoints	CW-CHW; ΔT_{db}	CW-CHW; ΔT_{db}	CW-CHW; ΔT_{db}
Parallel; Variable	CW-CHW; kW/ton^{*}_{CT}	CW-CHW; kW/ton^{*}_{CT}	CW-CHW; kW/ton^{*}_{CT}	CW-CHW; kW/ton^{*}_{CT}	CW-CHW; kW/ton^{*}_{CT}	CW-CHW; kW/ton^{*}_{CT}
Series; Variable	CHW; $kW/ton*_{CT}$	CHW; kW/ton^{*}_{CT}	CW-CHW; kW/ton^{*}_{CT} and dPLR	CHW; kW/ton^{*}_{CT}	CHW; kW/ton^{*}_{CT}	CHW; kW/ton^{*}_{CT}

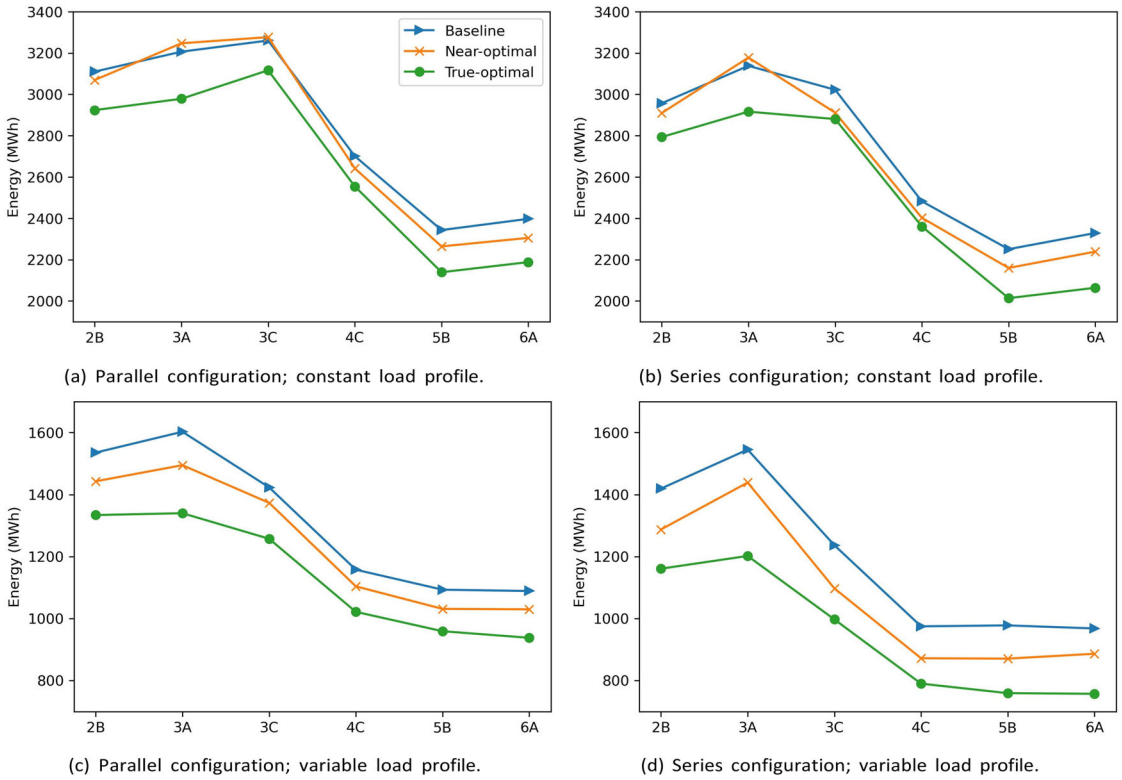

Fig. 12. Comparison of baseline, near-optimal, and true-optimal annual energy results.

Table 4 shows the recommended advanced control sequence category and optimization parameters to develop near-optimal control sequences for the chiller plants with WSE systems. The advanced control sequence category is chosen first based on energy performance, then FC hours if the energy performance is similar among two or more sequences. FC hours are included as a secondary metric since operating more in FC mode can prolong the lifecycle of expensive chillers. The optimization parameters are included if they offer significant energy savings and/or increase in FC hours and are otherwise excluded if they do not significantly improve these metrics. Minimizing the number of optimization parameters provides more practical sequences for chiller plant operators.

The CW-CHW sequence is recommended for the majority of the systems (except for most of the series configuration and variable load systems) because it is often the most energy efficient and/or increases FC hours. The CHW sequence is recommended for most of the series configuration and variable load systems because it was more energy efficient for those cases. Optimizing ΔT_{db} is recommended for many of the constant load cases because it can increase the FC hours and optimizing kW/ton^{*}_{CT} is recommended for the variable load systems because of its energy performance.

Figure 12 compares the baseline, near-optimal, and true-optimal energy results. The baseline values are the average values among the three sequences with default setpoints. The near-optimal results are based on the recommended sequences in Table 4 and the true-optimal results come from the hourly-level optimizations as described in Section 3.5.

Table 5. Optimized values of kW/ton^{*}_{CT} for the CW-CHW sequence.

Configuration/load profile	*2B*	*3A*	*3C*	*4C*	*5B*	*6A*
Parallel; Constant	0.10	0.05	0.10	0.10	0.10	0.10
Series; Constant	0.10	0.05	0.10	0.10	0.10	0.10
Parallel; Variable	0.03	0.03	0.04	0.04	0.04	0.03
Series; Variable	0.04	0.03	0.04	0.04	0.04	0.03

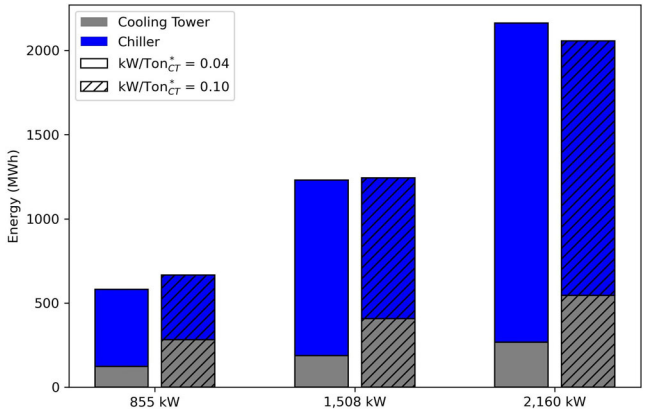

Fig. 13. Breakdown of annual cooling tower and chiller energy consumption for three different constant load values.

As expected, the near-optimal results never save more energy than the true-optimal results. This is because the hourly-level optimization of parameters for the true-optimal scenarios always outperforms the annual optimizations in the near-optimal scenarios. The near-optimal energy results are almost always lower than the baseline results, except for the constant load cases in climate 3A and the parallel configuration with constant load case in climate 3C. This is because all of the near-optimal sequences for the constant load cases use the CW-CHW sequence, but this sequence consumes slightly more energy than the other two sequences in climates 3A and 3C. Despite this, the CW-CHW sequence is recommended for two reasons: 1) it can significantly increase the FC hours with small differences in energy consumption and 2) providing uniform sequences (i.e., avoiding recommending different base advanced sequences and optimal parameters) can be more practical for operators.

4.2. Detailed analysis

Some of the key findings from the optimization results are explored in more detail in this section. First, the impacts of optimizing kW/ton^{*}_{CT} for the variable load profile systems are examined. Then, interesting results for the series configuration with variable load profiles are analyzed.

4.2.1. Optimizing kW/ton^{*}_{CT} for variable load systems

First, the results in Figure 9 show that optimizing kW/ton^{*}_{CT} can lead to significant energy savings for the variable load systems. Furthermore, the optimized values for kW/ton^{*}_{CT} in Figure 11b often follow a bimodal distribution with peaks around 0.10 and 0.04, which correspond to optimal values for constant and variable load profiles, respectively. A sample of these optimized values for different combinations of configuration, load profile, and climate is shown in Table 5. This sample only includes kW/ton^{*}_{CT} optimization in the CW-CHW sequence. Except for climate zone 3A, the optimized values follow the described bimodal distribution based on load profile.

This distribution pattern is due to the balance of cooling tower and chiller energy for different load values. To demonstrate this, we conducted a test of three constant load values (855 kW, 1,508 kW, and 2,160 kW) using two kW/ton^{*}_{CT} values (0.04 and 0.10). The tests are conducted for the parallel configuration plant using the CW-CHW sequence in climate zone 3 C. The three load values represent the minimum load value for the variable load profile in this climate, the maximum value of the variable load profile (which is the same in all climates and equal to the constant load profile value), and the average of those two values.

Figure 13 shows the breakdown of chiller and cooling tower energy consumption for these six scenarios. First, decreasing the value of kW/ton^{*}_{CT} shifts the energy consumption from the cooling tower to the chiller because a lower value of kW/ton^{*}_{CT} means the CWST setpoint resets when the cooling tower is operating at a more efficient threshold. When the load is smaller, the chiller can handle the majority of the load and the system operates more efficiently by using less cooling tower energy. Conversely,

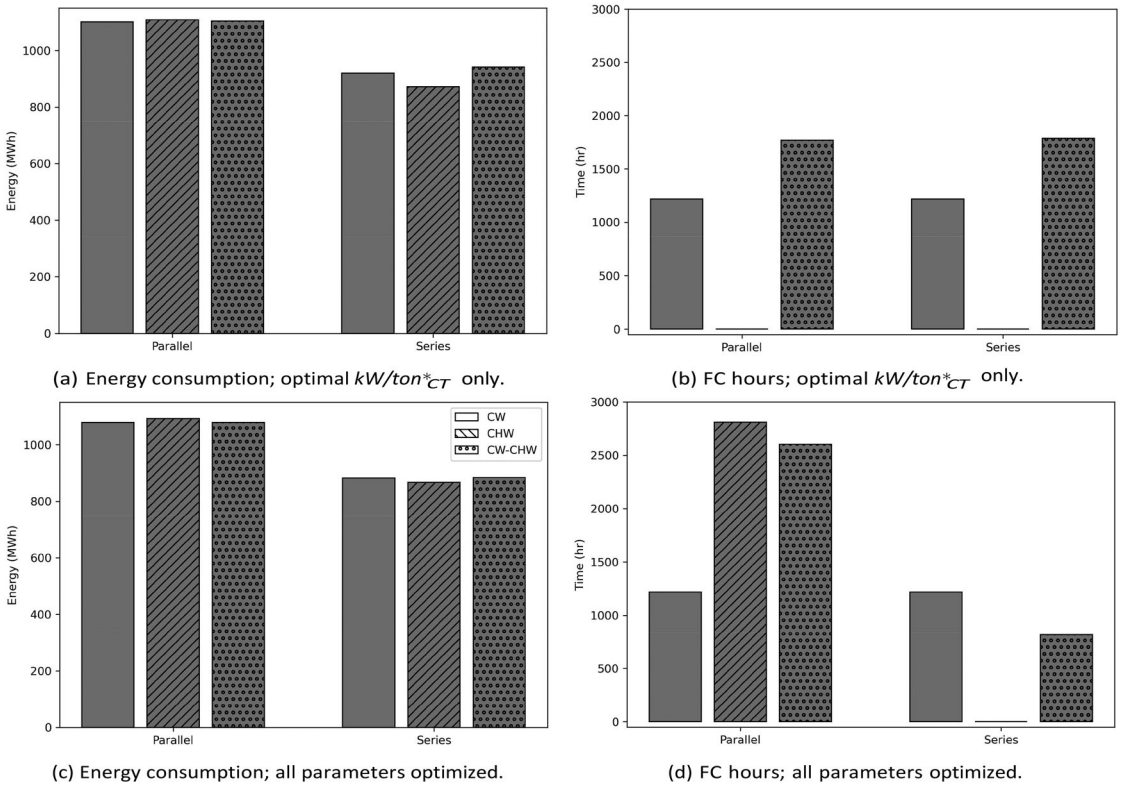

Fig. 14. Optimized energy results and FC hours for the variable load profile chiller plants with WSE systems in climate 4C.

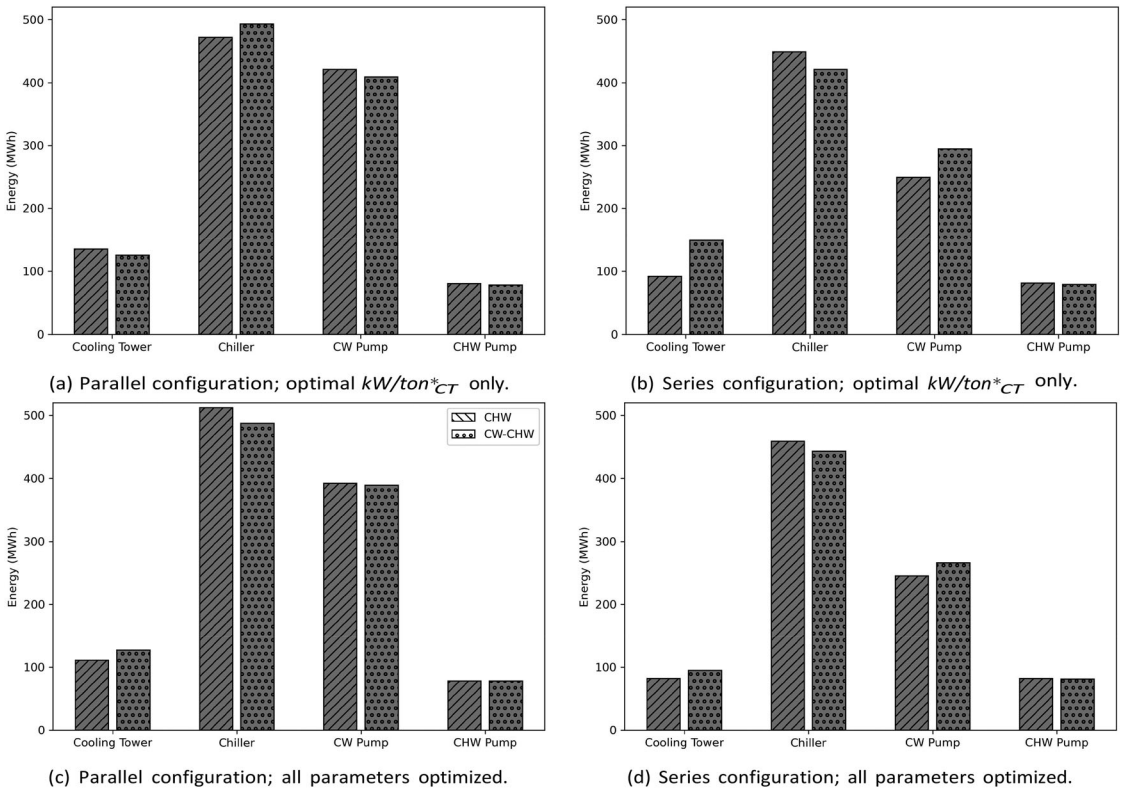

Fig. 15. Breakdown of optimized energy results for the variable load profile chiller plants with WSE systems in climate 4C.

relying more on the cooling tower is relatively efficient when the load is higher. Thus, the optimal value of kW/ton^*_{CT} is lower for the variable load profiles because the load is smaller compared to the constant load cases. These results are dependent on the size and performance curves of equipment such as chillers and cooling tower fans.

4.2.2. Series configuration and variable load profile analysis The previous results showed unique findings for the series configuration and variable profile load cases. Specifically, the CHW sequence often offered the best energy savings by reducing the FC hours for these systems in the colder climates. This is counter-intuitive because oftentimes increasing the FC hours reduces the energy consumption.

The following results expand on these findings by analyzing the effects of free cooling and chiller plant configuration on chiller plant energy efficiency. First, Figure 14 shows the energy consumption and FC hours for the variable load profile cases in climate 4 C when optimizing only kW/ton^*_{CT} (which provides the majority of the energy savings) and when optimizing all three parameters. Although optimizing all three parameters leads to energy savings by increasing the number of FC hours in the parallel CHW and CW-CHW scenarios, energy savings were attained by decreasing the number of FC hours in the series CW-CHW scenario. Furthermore, the CHW sequence is the most energy efficient for the series configuration despite having close to zero FC hours. These findings suggest the system does not always operate more efficiently in FC mode.

A breakdown of the energy consumption components for the variable load profile systems in climate 4 C is shown in Figure 15. The CHW and CW-CHW sequences are compared in these plots for the optimal kW/ton^*_{CT} and all optimized parameter cases. Optimizing all three parameters for the parallel configuration with CW-CHW sequence saves energy by increasing the FC hours. Although the number of FC hours increases for the parallel configuration with CHW sequence, the chiller energy also increases because of a lower optimized value of kW/ton^*_{CT}. Optimizing all three parameters for the series configuration with CW-CHW sequence reduces the FC hours to provide energy savings from the CW pump and cooling tower. Similarly, the CHW sequence is the most efficient sequence for the series configuration case despite using almost zero FC hours due to the cooling tower and CW pump's lower energy use. This is because, for this particular system type (series configuration and variable load profile), the system often operates more efficiently in PMC mode rather than FC mode by using only one CW pump and shifting some of the load from the cooling tower to the chiller.

5. Conclusion

This paper proposed a method to develop near-optimal control sequences for chiller plants with WSEs. First, advanced control sequences for chiller plants with WSE were identified and critical control parameters were optimized for those sequences. The critical control parameters included a cooling tower efficiency to reset the CWST for a new CWST control, a dead band temperature to switch between different control modes, and chiller differential part load ratio to determine when to stage additional chillers on/off. The control parameters were optimized alone and in combination with each other for systems with two configurations, two load profiles, three identified advanced control sequences, and six climates. Finally, the near-optimal sequences for each combination of system configuration, load profile, and climate are determined based on the optimization results. These sequences provide guidance to operators for implementing advanced control sequences without the need to develop and integrate complex system models.

The results show the recommended near-optimal sequences can reduce energy consumption by up to 15% relative to the baseline depending on the configuration, load profile, and climate. Specifically, the CW-CHW sequence is recommended for the majority of systems (except most of the series configuration with variable load profile systems) because it is often the most energy efficient and/or increases FC hours. Optimizing ΔT_{db} is recommended for many of the constant load systems because it can increase FC hours and optimizing kW/ton^*_{CT} in the CWST reset control is recommended for the variable load systems because of its energy performance. Lastly, the results showed reducing the number of FC hours can provide energy savings for the series configuration and variable load profile systems in colder climates by using less CW pump energy and shifting cooling burden from the cooling towers to the chillers. These findings provide practical guidance for operators to improve the operation of chiller plants with WSEs.

Future work can be conducted based on this paper. First, three representative advanced control sequences were selected for this study, but newer advanced controls can be applied using this methodology. Other critical control parameters, such as those relating to pump controls, can be optimized as well. Also, the results in this paper are specific to the studied systems and the performance curves of their components. Studying other system types or sizes with different performance curves can help quantify those parameters' impacts on control optimization for chiller plants with WSEs. Finally, this paper focused on optimizing the systems to minimize plant energy consumption. Future work can examine optimizing life cycle costs such as considering the life cycle of chillers when utilizing WSEs.

Acknowledgements

The authors want to the thank the TRP-1661 Project Monitoring Subcommittee (Keith Cockerham, Tim McDowell, Li Song, and Jeff Stein) for their valuable guidance during the project.

Disclosure statement

No potential conflict of interest was reported by the author(s).

Funding

This paper is the outcome of the research project TRP-1661 sponsored by American Society of Heating, Refrigerating and Air-Conditioning Engineers (ASHRAE).

References

Agrawal, A., M. Khichar, and S. Jain. 2016. Transient simulation of wet cooling strategies for a data center in worldwide climate zones. *Energy and Buildings* 127:352–9. doi:10.1016/j.enbuild.2016.06.011

ASHRAE. 2023, RP-1661 – Development of near-optimal control sequence for chiller plants with water side economizers using dynamic models.

Carrier Corporation. 2016. How to model a waterside economizer application. *Carrier Engineering Newsletter* 4 (1):1–16.

Cho, J., and Y. Kim. 2016. Improving energy efficiency of dedicated cooling system and its contribution towards meeting an energy-optimized data center. *Applied Energy* 165:967–82. doi:10.1016/j.apenergy.2015.12.099

Comperchio, D., and S. Behere. 2015. Theoretical and empirical energy impacts of economization in data centers. doi:doi:10.1115/IPACK2015-48274.

Durand-Estebe, B., C. Le Bot, J. N. Mancos, and E. Arquis. 2014. Simulation of a temperature adaptive control strategy for an IWSE economizer in a data center. *Applied Energy* 134:45–56. doi:10.1016/j.apenergy.2014.07.072

Energy Information Administration. 2023. Degree days.

Energy Star. 2024. Consider water side economizers. https://www.energystar.gov/products/consider_water_side_economizers.

Fan, C., and X. Zhou. 2023. Model-based predictive control optimization of chiller plants with water-side economizer system. *Energy and Buildings* 278:112633. doi:10.1016/j.enbuild.2022.112633

Fan, C., K. Hinkelman, Y. Fu, W. Zuo, S. Huang, C. Shi, N. Mamaghani, C. Faulkner, and X. Zhou. 2021. Open-source modelica models for the control performance simulation of chiller plants with water-side economizer. *Applied Energy* 299:117337. doi:10.1016/j.apenergy.2021.117337

Ganguly, S., S. Raje, S. Kumar, D. Sartor, and S. Greenberg. 2016. *Accelerating energy efficiency in Indian data centers. Final report for phase I activities*. Technical Report. Lawrence Berkeley National Lab.(LBNL), Berkeley, CA (United States).

Greeley, D. 2006. The winter efficiency protagonist: Best practice for a partial waterside economizer. *Engineered Systems* 23:68–76.

Griffin, B. 2015a. Data center economizer efficiency. *ASHRAE Journal* 57:64–70.

Griffin, B. 2015b. Honorable mention: Industrial facilities or processes, new data center: Economizer efficiency. *ASHRAE Journal* 57:64–9.

Ham, S., and J. W. Jeong. 2016. Impact of aisle containment on energy performance of a data center when using an integrated water-side economizer. *Applied Thermal Engineering* 105:372–84. doi:10.1016/j.applthermaleng.2015.05.069

Han, X., W. Tian, J. VanGilder, W. Zuo, and C. Faulkner. 2021. An open source fast fluid dynamics model for data center thermal management. *Energy and Buildings* 230:110599. doi:10.1016/j.enbuild.2020.110599.

Huang, S., W. Zuo, and M. D. Sohn. 2017. Improved cooling tower control of legacy chiller plants by optimizing the condenser water set point. *Building and Environment* 111:33–46. doi:10.1016/j.buildenv.2016.10.011

Jaramillo, R., B. Jeon, and D. Schuster. 2015. Simulation assessment of free-cooling technology for a large campus.

Kim, J. Y., H. J. Chang, Y. H. Jung, K. M. Cho, and G. Augenbroe. 2017. Energy conservation effects of a multi-stage outdoor air enabled cooling system in a data center. *Energy and Buildings* 138:257–70. doi: doi:10.1016/j.enbuild.2016.12.057.

Kim, Y. J., J. W. Ha, K. S. Park, and Y. H. Song. 2021. A study on the energy reduction measures of data centers through chilled water temperature control and water-side economizer. *Energies* 14 (12):3575. doi:10.3390/en14123575.

Li, J., and Z. Li. 2020. Model-based optimization of free cooling switchover temperature and cooling tower approach temperature for data center cooling system with water-side economizer. *Energy and Buildings* 227:110407. doi:10.1016/j.enbuild.2020.110407

Li, P., Y. Li, J. E. Seem, H. Qiao, X. Li, and J. Winkler. 2014. Recent advances in dynamic modeling of HVAC equipment. Part 2: Modelica-based modeling. *HVAC&R Research* 20 (1):150–61. doi:10.1080/10789669.2013.836876

Liu, Z., H. Tan, D. Luo, G. Yu, J. Li, and Z. Li. 2017. Optimal chiller sequencing control in an office building considering the variation of chiller maximum cooling capacity. *Energy and Buildings* 140:430–42. doi:10.1016/j.enbuild.2017.01.082.

Lui, Y. 2010. Waterside and airside economizers design considerations for data center facilities.

MacQueen, J. 1997. Modelling and simulation of energy management control system. Ph.D. thesis. University of Strathclyde.

Meakins, M. E. 2011. *Energy and exergy analysis of data center economizer systems*. San Jose State University. doi:10.31979/etd.bf7d-khxd.

Moser, I. 2009. Hooke-jeeves revisited. *2009 IEEE Congress on Evolutionary Computation* 2670–6. https://api.semanticscholar.org/CorpusID:26488308.

Park, C., D. R. Clark, and G. E. Kelly. 1985. An overview of HVACSIM+, a dynamic building/HVAC/control systems simulation program. In *Proceedings of the 1st Annual Building Energy Simulation Conference*, Seattle, WA, 21–2.

Seo, B., and K. Lee. 2016. Detailed analysis on part load ratio characteristics and cooling energy saving of chiller staging in an office building. *Energy and Buildings* 119:309–22. doi:10.1016/j.enbuild.2016.03.067.

Stein, J. 2009. Waterside economizing in data centers: Design and control considerations. *ASHRAE Transactions* 115–92.

Stull, R. 2011. Wet-bulb temperature from relative humidity and air temperature. *Journal of Applied Meteorology and Climatology* 50 (11):2267–9. doi: doi:10.1175/JAMC-D-11-0143.1.

Taylor, S. T. 2014. How to design & control waterside economizers. *ASHRAE Journal* 56:30–6.

Taylor, S. T. 2015. Resetting setpoints using trim & respond logic. *Ashrae Journal* 57:52–7.

Udagawa, Y., S. Waragai, M. Yanagi, and W. Fukumitsu. 2010. Study on free cooling systems for data centers in japan. Intelec 2010, 1–5. doi:10.1109/INTLEC.2010.5525676.

Wetter, M., W. Zuo, T. Nouidui, and X. Pang. 2014. Modelica buildings library. *Journal of Building Performance Simulation* 7 (4):253–70. doi:10.1080/19401493.2013.765506.

Zhang, H., S. Shao, H. Xu, H. Zou, and C. Tian. 2014. Free cooling of data centers: A review. *Renewable and Sustainable Energy Reviews* 35:171–82. doi:10.1016/j.rser.2014.04.017